Journal of Elasticity
https://doi.org/10.1007/s10659-022-09951-y

On the Stability of Surface Growth: The Effect of a Compliant Surrounding Medium

Rohan Abeyaratne[1] · **Eric Puntel**[2] · **Giuseppe Tomassetti**[3]

Dedicated with admiration to Roger L. Fosdick

Received: 29 July 2022 / Accepted: 28 October 2022

Abstract
In a recent paper Abeyaratne et al. (J. Mech. Phys. Solids 167:104958, 2022) concerning the stability of surface growth of a pre-stressed elastic half-space with surface tension, it was shown that steady growth is never stable, at least not for all wave numbers of the perturbations, when the growing surface is traction-free. On the other hand, steady growth was found to be always stable when growth occurred on a flat frictionless rigid support and the stretch parallel to the growing surface was compressive. The present study is motivated by these somewhat unexpected and contrasting results.

In this paper the stability of a pre-compressed neo-Hookean elastic half-space undergoing surface growth under plane strain conditions is studied. The medium outside the growing body resists growth by applying a pressure on the growing surface. At each increment of growth, the incremental change in pressure is assumed to be proportional to the incremental change in normal displacement of the growing surface. It is shown that surface tension stabilizes a homogeneous growth process against small wavelength perturbations while the compliance of the surrounding medium stabilizes it against large wavelength perturbations. Specifically, there is a critical value of stretch, $\lambda_{cr} \in (0, 1)$, such that growth is linearly stable against infinitesimal perturbations of *arbitrary* wavelength provided the stretch parallel to the growing surface exceeds λ_{cr}. This *stability threshold*, λ_{cr}, is a function of the non-dimensional parameter $\sigma\kappa/G^2$, which is the ratio between two length-scales σ/G and G/κ, where G is the shear modulus of the elastic body, σ is the surface tension, and κ is the stiffness of the surrounding compliant medium.

It is shown that (a) $\lambda_{cr} \to 1$ as $\kappa \to 0$ and (b) $\lambda_{cr} \to 0^+$ as $\kappa \to \infty$, thus recovering the results in Abeyaratne et al. (J. Mech. Phys. Solids 167:104958, 2022) pertaining to the respective limiting cases where growth occurs (a) on a traction-free surface and (b) on a frictionless rigid support. The results are also generalized to include extensional stretches.

Keywords Surface growth · Surface stability · Surface tension · Stiffness · Compliant medium · Actin · Biot instability

Mathematics Subject Classification (2020) 74A15 · 74B20 · 92C05

Extended author information available on the last page of the article

1 Introduction

1.1 Surface Growth Is Ubiquitous

Surface growth – the addition of new material to the surface of a solid body – occurs in a variety of contexts, perhaps the most familiar being the solidification of water on the surface of an ice cube below the freezing temperature. Other examples include 3D-printing, chemical vapor deposition, the growth of hard tissue like bone, and the polymerization of actin networks in the cytoskeleton of a biological cell.

1.2 Compliant Resistance to Surface Growth

Actin polymerization plays a central role in cell biology; see, for example, the review articles [5], [26], [32] and the references therein. In a series of intriguing experiments, Parekh et al. [30], Chaudhuri et al. [12] and Bieling et al. [7], polymerized an actin network between an AFM (atomic force microscope) cantilever and a fixed surface. One end of the cantilever was functionalized with an actin nucleating agent and this led to polymerization at that end. Once the growing actin network reached the fixed surface, it pushed against the cantilever during further growth, with the elasticity of the cantilever providing a *compliant resistance* to growth. Similarly, an actin network growing inside a cell pushes against the cell membrane which provides a compliant resistance to growth.

1.3 Instability of Surface Growth

Surface instability is well-known in materials science where growing surfaces can become unstable due to a coupling between growth and stress, e.g., Mullins and Serkeka [27], Asaro and Tiller [6] and Grinfeld [19].

Symmetry-breaking instabilities are frequently encountered in biology during surface growth. An example of this was seen in the striking experiments of Noireaux et al. [29], Cameron et al. [11] and others in which they chemically treated the surface of a micron-size rigid bead immersed in a solution of free actin monomers. The actin monomers were attracted to the surface of the bead where they polymerized and attached onto the actin network growing around the bead. Each newly formed layer of solid at the bead surface pushed out the previously formed solid which induced stress in the network; for modeling of this spherically symmetric growth process see Noireaux et al. [29], Dafalias et al. [14], [15] and Tomassetti et al. [35]. When the growing actin shell reached a certain critical thickness it lost spherical symmetry and developed a "comet tail"; see van der Gucht et al. [20]; Prost et al. [31]; and John et al. [23].

1.4 Continuum Mechanical Modeling of Surface Growth

The addition of new material points to the surface of a growing body leads to a time-dependent reference configuration, with the evolution of the reference configuration being intimately tied to the accretive growth of the body. Modeling this is challenging. Inspired by the seminal paper of Skalak et al. [33], some progress was made by Tomassetti et al. [35] when the geometry is simple, e.g., one dimensional, planar or cylindrically/spherically symmetric. An alternative Eulerian approach, which seeks to by-pass consideration of the reference configuration, has been developed by Naghibzadeh et al. [28].

The growth process itself is characterized by a kinetic law relating the propagation speed of the boundary in the reference configuration (which is a measure of the rate at which new material is added to the body) and a power conjugate thermodynamic driving force.

1.5 A Recent Study

In a recent paper [4], we examined the stability of steady surface growth of a pre-stressed elastic half-space with surface tension. While several mechanical boundary conditions at the growing surface were considered, the two of interest to us here are (*a*) the case where the growing surface is traction-free, and (*b*) the case where growth occurs on a flat frictionless rigid support. These cases were motivated by the boundary conditions at (*a*) the outer and (*b*) the inner surfaces of the actin shell growing around a bead mentioned above. By constructing steady solutions and examining their linearized stability, we showed that the steady solution in the former case, (*a*), is never stable, at least not for all wave numbers of the perturbations, and that it is always stable in the latter case (*b*) when the stretch parallel to the growth surface is compressive. The present study was motivated by these somewhat unexpected and contrasting results.

In the absence of growth, the problem studied in [4] is the classical Biot instability problem for a half-space, albeit with somewhat more general boundary conditions. In the most familiar case, where the boundary of the half-space is traction-free and surface tension is ignored, Biot [8] showed that the body became unstable through a surface instability when the stretch parallel to the boundary reached the value λ_{Biot} (≈ 0.5437) given by the unique real, positive root of the polynomial equation $\lambda^6 + \lambda^4 + 3\lambda^2 - 1 = 0$. In such a surface instability mode, the infinitesimal deformation superposed on the homogeneous one involves periodic oscillations parallel to the boundary and exponential decay away from it. There is a substantial literature on various questions and generalizations of this problem, e.g., the stability of the deformation[1] [13]; generalization beyond the neo-Hookean model to arbitrary incompressible isotropic materials [16]; the rich phenomena seen beyond plane strain [34]; generalization to hydrogels [24]; loading by electrostatic stress [22]; and so on.

1.6 The Present Study and Its Key Results

In the present study we again consider the growth of a pre-stressed neo-Hookean half-space, but now allow the medium outside the body to be compliant and to afford some resistance to growth. Specifically, the medium on the outside is assumed to apply a pressure on the boundary of the growing body such that, at each increment of growth, the incremental change in pressure is proportional to the incremental change in normal displacement of the growing surface. This was motivated in part by the examples described previously in Sect. 1.2, and by the simple fact that our previous study [4] corresponds to the limiting cases of a compliant environment when its stiffness tends (*a*) to zero and (*b*) to infinity respectively.

We first construct a time-dependent spatially homogeneous growth process conforming to the boundary-initial value problem, that for brevity, we refer to as a "homogeneous solution". During such a growth process, the deformation is spatially homogeneous and time-independent, but the body undergoes an unsteady *time-dependent* evolution. This is because when, for example, the driving force for growth is positive at the initial instant, the body starts to grow through accretion at its boundary. As it grows, the boundary moves outwards and so the pressure applied on it by the surrounding medium increases. As the pressure increases, the driving force decreases, and so does the rate of growth. Eventually, as $t \to \infty$, the driving force vanishes, growth stalls, and the body reaches equilibrium.

Next, we study the linearized stability of a homogeneous solution and show that there is a critical stretch $\lambda_{\text{cr}} \in (0, 1)$ such that growth is stable when the *compressive* stretch parallel

[1] Biot's analysis shows that the problem has a second solution close to the homogeneous one when $\lambda = \lambda_{\text{Biot}}$ but does not, strictly, address stability.

to the boundary of the body is greater than this value. There are two length-scales in the problem, σ/G and G/κ where G is the shear modulus of the neo-Hookean elastic body, σ the surface tension and κ the stiffness of the surrounding medium. We show that the *stability threshold* $\lambda_{\rm cr}$ is a function of the nondimensional parameter $\sigma\kappa/G^2$ that is the ratio of these two length-scales. Moreover, we find that $\lambda_{\rm cr} \to 1$ as $\kappa \to 0$ and $\lambda_{\rm cr} \to 0^+$ as $\kappa \to \infty$, thus recovering the aforementioned results in [4] as special cases.

In Appendix C we generalize these results to include extensional stretches. It is shown there that in general there are two critical values of stretch, $\lambda_{\rm cr}^{\pm}$, which demarcate the range of stability. The stretch $\lambda_{\rm cr}^{-} \in (0, 1)$ is compressive (and coincides with the stretch $\lambda_{\rm cr}$ referred to above) while $\lambda_{\rm cr}^{+} \in (1, 1/\lambda_{\rm Biot})$ is extensional. The homogeneous solution is stable against all perturbations when the stretch parallel to the free surface lies between these two critical values of stretch. The stretch $\lambda_{\rm cr}^{+} \to 1$ when $\kappa \to 0$ and $\lambda_{\rm cr}^{+} \to 1/\lambda_{\rm Biot}$ when $\kappa \to \infty$.

1.7 Organization of the Rest of the Paper

The basic equations pertaining to the problem of interest are presented in the preliminary Sect. 2. Next, in Sect. 3, we specialize the field equations and boundary conditions to a semi-infinite neo-Hookean body whose boundary is a flat plane. We then construct a homogeneous solution to the problem which, as already mentioned, involves a homogeneous time-independent deformation but a non-steady time-dependent evolution of stress, driving force and boundary location. Thereafter, in Sect. 4, we perturb the homogeneous solution, keeping in mind that as part of perturbing the solution, one must also perturb the domain on which it is defined, i.e., the reference configuration. This is related to the fact that the problem at hand is a free boundary-initial value problem and the (time-dependent) domain of the solution is one of the unknowns. An inhomogeneous time-dependent process is now considered and linearized about the homogeneous solution. This leads to the linearized problem. Finally in Sect. 5 we analyze the linearized problem with a focus on the question of whether perturbations grow or decay with time. In Appendix A we establish some formulae used elsewhere and in Appendix B we derive the expression for the driving force in the presence of both the boundary pressure and surface tension. The results of this paper are generalized to include extensional stretches in Appendix C.

2 Preliminaries

We will be concerned with plane strain throughout and will not need to refer to the out-of-plane components of vector and tensor fields.

In the reference configuration, the body occupies a *time-dependent* (two-dimensional) region $\mathcal{R}_{\rm R}(t)$ that is bounded by the curve $\mathcal{S}_{\rm R}(t)$. Because we are allowing for surface growth, i.e., the addition of material particles to the body at $\mathcal{S}_{\rm R}(t)$, the region $\mathcal{R}_{\rm R}(t)$ and its boundary $\mathcal{S}_{\rm R}(t)$ will be time-dependent in general.

At each instant t during an evolution process, the particle located at $\boldsymbol{\xi}$ in the reference configuration is mapped to the position $\mathbf{y}(\boldsymbol{\xi}, t)$ in the current configuration. In the current configuration the body occupies the region $\mathcal{R}(t) = \mathbf{y}(\mathcal{R}_{\rm R}(t), t)$ that is bounded by the curve $\mathcal{S}(t) = \mathbf{y}(\mathcal{S}_{\rm R}(t), t)$. The regions occupied by the body in the reference and current configurations, and their boundaries, are shown schematically in Fig. 1. We denote the unit outward normal vectors on $\mathcal{S}_{\rm R}$ and $\mathcal{S}$ by $\mathbf{n}_{\rm R}$ and $\mathbf{n}$ respectively.

The motion of the boundary $\mathcal{S}_{\rm R}(t)$ in the reference configuration is solely due to surface growth, and when we characterize the kinetics of surface growth below, we will make use

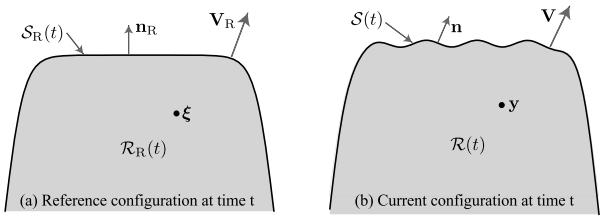

Fig. 1 Schematic depiction of the time-dependent regions $\mathcal{R}_{\mathrm{R}}(t)$ and $\mathcal{R}(t)$ occupied by a body in the reference and current configurations and their boundaries $\mathcal{S}_{\mathrm{R}}(t)$ and $\mathcal{S}(t)$. The velocities of points on the moving curves $\mathcal{S}_{\mathrm{R}}(t)$ and $\mathcal{S}(t)$ are $\mathbf{V}_{\mathrm{R}}$ and $\mathbf{V}$, and the unit outward normal vectors are $\mathbf{n}_{\mathrm{R}}$ and $\mathbf{n}$. The body is surrounded by a compliant medium

of the propagation speed $\mathbf{V}_{\mathrm{R}} \cdot \mathbf{n}_{\mathrm{R}}$ of $\mathcal{S}_{\mathrm{R}}$. On the other hand, the motion of the boundary $\mathcal{S}(t)$ in the current configuration is due to both growth and deformation. As the body grows and the curve $\mathcal{S}(t)$ moves outwards, it pushes against the surrounding medium which we assume applies a pressure on the growing body. In order to characterize this mechanical boundary condition we will need the propagation speed $\mathbf{V} \cdot \mathbf{n}$ of $\mathcal{S}(t)$. When speaking of velocities, it is important to distinguish between the velocities of points that move with these curves and the velocity $\mathbf{v}$ of the material particle that is instantaneously located on the boundary. The relation between them can be derived by differentiating $\mathbf{y}_*(t) = \mathbf{y}(\boldsymbol{\xi}_*(t), t)$ with respect to time where $\boldsymbol{\xi}_*(t)$ and $\mathbf{y}_*(t)$ are corresponding points on the propagating surfaces $\mathcal{S}_{\mathrm{R}}(t)$ and $\mathcal{S}(t)$. This leads to

$$\mathbf{V} = \mathbf{F}\mathbf{V}_{\mathrm{R}} + \mathbf{v}, \tag{1}$$

where $\mathbf{v} = \partial \mathbf{y}(\boldsymbol{\xi}, t)/\partial t$ is particle velocity and

$$\mathbf{F} := \mathrm{grad}_{\boldsymbol{\xi}} \mathbf{y} \tag{2}$$

is the deformation gradient tensor. In the absence of growth $\mathbf{V}_{\mathrm{R}} = \mathbf{o}$, and therefore $\mathbf{V} = \mathbf{v}$ as usual.

The dissipation rate associated with surface growth can be shown to be $f V_{\mathrm{R}}$ where

$$f := \Delta\mu + \mathbf{S}\mathbf{n}_{\mathrm{R}} \cdot \mathbf{F}\mathbf{n}_{\mathrm{R}} - W(\mathbf{F}) \tag{3}$$

is the thermodynamic driving force and $V_{\mathrm{R}} = \mathbf{V}_{\mathrm{R}} \cdot \mathbf{n}_{\mathrm{R}}$ is the propagation speed of the referential boundary. Here $\Delta\mu > 0$ is the difference between the chemical energy (per unit reference volume) of a free material particle unattached to the growing body and that of a material particle bound to the body; $\mathbf{S}$ is the Piola stress and $W(\mathbf{F})$ is the strain energy density. A derivation of (3) is sketched in Appendix B, generalizing the calculation of Tomassetti et al. [35] to include both the pressure loading and surface tension.

In general irreversible processes, driving forces and their conjugate fluxes are identified from the dissipation (entropy-production) rate, and the kinetics of such processes are then taken to be characterized by relations between these fluxes and driving forces; see for example Chap. 14 of Callen [10], Chap. 14 of Kestin [25], and Abeyaratne and Knowles [1], [2], [3]. Following this approach, we assume the kinetics of surface growth to be described by a relation between the normal growth speed V_{R} and the conjugate driving force f:

$$V_{\mathrm{R}} = \mathsf{V}(f). \tag{4}$$

Note that this is essentially a kinetic law for the mass flux $\rho_{\rm R} V_{\rm R}$ associated with growth where $\rho_{\rm R}$ is the referential mass density. The kinetic response function $\mathsf{V}(f)$ characterizes growth and the dissipation inequality $f V_{\rm R} \geq 0$ requires that $\mathsf{V}(f) f \geq 0$. We shall assume $\mathsf{V}(f)$ to be monotonically increasing with $\mathsf{V}(0) = 0$:

$$\mathsf{V}'(f) > 0, \quad \mathsf{V}(0) = 0. \tag{5}$$

Thus, the larger the driving force, the faster the growth. When $f > 0$ the speed $V_{\rm R} > 0$ and so the boundary $\mathcal{S}_{\rm R}$ moves outwards and material is added to the body (accretion); when $f < 0$ the speed $V_{\rm R} < 0$ and so $\mathcal{S}_{\rm R}$ moves inwards and material is removed from the body (ablation). There is no growth at zero driving force.

We now turn to the mechanical boundary condition. In the experiments described in [30], [12] and [7], the authors grew an actin network between an AFM cantilever and a fixed surface where the growth was resisted by the elasticity of the cantilever. Likewise, when an actin network grows inside a cell during cell locomotion, the growth is resisted by the compliant cell wall. Motivated by these examples, suppose that the growing body here is surrounded by a compliant medium that applies a pressure on the boundary $\mathcal{S}(t)$ as it moves outwards. The increment of pressure is assumed to be linearly related to the increment of normal displacement of the boundary, and so, in the absence of surface tension, we would take the boundary condition on $\mathcal{S}(t)$ to be

$$\mathbf{T}\mathbf{n} = -p\mathbf{n} \quad \text{where} \quad \dot{p} = \kappa \mathbf{V} \cdot \mathbf{n}.$$

Here $\mathbf{T}$ is the Cauchy stress tensor and the constant parameter $\kappa > 0$ is the stiffness of the surrounding medium. In order to account for surface tension, let $\mathbf{T}^+\mathbf{n}$ and $\mathbf{T}^-\mathbf{n}$ denote the limiting values of Cauchy traction on either side of $\mathcal{S}(t)$, with plus denoting the outside of the growing body. Then

$$\mathbf{T}^+\mathbf{n} - \mathbf{T}^-\mathbf{n} = -\sigma \varkappa \mathbf{n} - \frac{\partial \sigma}{\partial s}\mathbf{t}, \tag{6}$$

where $\sigma > 0$ denotes the surface tension on the boundary, $\mathbf{t}$ is the unit tangent vector in the direction of increasing arc length s, and $\varkappa$ is the curvature of $\mathcal{S}(t)$; see for example [9]. In the setting we have in mind here, $\mathbf{T}^+\mathbf{n} = -p\mathbf{n}$ on the outside and $\mathbf{T}^- = \mathbf{T}$ is the limiting stress from within the solid body. Combining this with the two preceding equations yields the following mechanical boundary condition:

$$\mathbf{T}\mathbf{n} = -p\mathbf{n} + \sigma \varkappa \mathbf{n} + \frac{\partial \sigma}{\partial s}\mathbf{t} \quad \text{where} \quad \dot{p} = \kappa \mathbf{V} \cdot \mathbf{n}. \tag{7}$$

The surface tension is assumed to obey the constitutive relation

$$\sigma = \mathcal{W}'(\lambda), \tag{8}$$

where $\lambda = 1/|\mathbf{F}^{-1}\mathbf{t}|$ is the stretch along the boundary and $\mathcal{W}(\lambda)$ is the surface energy per unit reference area (per unit reference length in plane strain). We remark that even though σ and $\mathcal{W}$ do not appear explicitly in (3), the model does account for surface tension; see Appendix B.

Finally, the Piola and Cauchy stress tensors satisfy the equilibrium equations,

$$\mathrm{div}_{\boldsymbol{\xi}} \mathbf{S} = \mathbf{o}, \quad \mathrm{div}_{\mathbf{y}} \mathbf{T} = \mathbf{o}, \tag{9}$$

having neglected body forces. They also obey the constitutive relations

$$\mathbf{S} = \frac{\partial W}{\partial \mathbf{F}} - q\,\mathbf{F}^{-T}, \quad \mathbf{T} = \frac{\partial W}{\partial \mathbf{F}}\mathbf{F}^{T} - q\,\mathbf{I}, \tag{10}$$

for an incompressible elastic solid. Here q is the reactive pressure and incompressibility requires

$$\det \mathbf{F} = 1. \tag{11}$$

Given the strain energy function $W(\mathbf{F})$, the surface energy function $\mathcal{W}(\lambda)$, the kinetic response function $\mathsf{V}(f)$, the stiffness κ and suitable initial conditions, the problem at hand requires us to determine the region $\mathcal{R}_{\mathrm{R}}(t)$, the motion $\mathbf{y}(\boldsymbol{\xi}, t)$ and the stress $\mathbf{T}(\mathbf{y}, t)$ conforming to the field equations (2), (9), (10), (11), and boundary conditions (4), (7).

In the rest of this paper we will limit attention to an incompressible neo-Hookean solid. In this case the strain energy function is

$$W(\mathbf{F}) = \frac{G}{2}\big(|\mathbf{F}|^2 - 2\big), \tag{12}$$

where the constant parameter $G > 0$ is the infinitesimal shear modulus, and the constitutive relations (10) for the Piola and Cauchy stresses specialize to

$$\mathbf{S} = G\,\mathbf{F} - q\,\mathbf{F}^{-T}, \quad \mathbf{T} = G\,\mathbf{F}\mathbf{F}^{T} - q\,\mathbf{I}. \tag{13}$$

Moreover, we limit attention to the case of constant surface tension σ where $\mathcal{W}(\lambda) = \sigma\lambda$.

3 Spatially Homogeneous Time-Dependent Growth Process

We now specialize the problem described in Sect. 2 to the case where the body is semi-infinite, the material neo-Hookean, the boundary $\mathcal{S}_{\mathrm{R}}(t)$ a straight line, and the deformation spatially homogeneous and time-independent.

It is worth pointing out at the outset that, even though the deformation is time-independent, the body undergoes an unsteady time-dependent process in general. This is because, as mentioned earlier, when for example the driving force for growth is positive at the initial instant, the body starts to grow through accretion on the boundary. As it grows, $\mathcal{S}(t)$ moves outwards and so the pressure applied on it by the surrounding medium increases. As the pressure increases, the driving force decreases, and so does the rate of growth. Eventually, as $t \to \infty$, the driving force vanishes, growth stalls, and the body reaches equilibrium. Note that the stress is time-dependent during this process through the reactive pressure $q(t)$ though the deformation is not. For simplicity, we will refer to this spatially homogeneous growth process as the "homogeneous solution".

In order to distinguish between the various quantities in this section and their inhomogeneous counterparts in Sect. 4, mathematical precision requires that we use different symbols for them. However, in order to avoid a vast amount of notation, we will avoid doing this as much as possible, and hope that the context makes clear as to what we are referring to. There will be a handful of exceptions: in the homogeneous solution in this section, we shall append a zero to the reactive pressure q_0, the pressure p_0 applied on the boundary by the surrounding medium, and the driving force f_0.

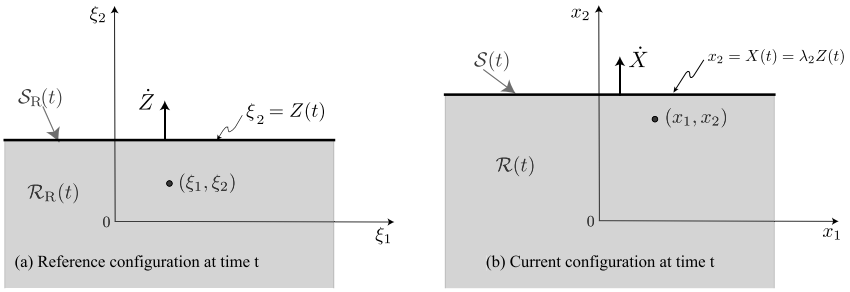

Fig. 2 Homogeneous solution: (a) The region $\mathcal{R}_{\rm R}(t)$ associated with the reference configuration at time t, and (b) the corresponding region $\mathcal{R}(t)$ associated with the current configuration. Note that the corresponding boundaries $\mathcal{S}_{\rm R}(t)$ and $\mathcal{S}(t)$ have propagation velocities $\dot{Z}\mathbf{e}_2$ and $\dot{X}\mathbf{e}_2$ respectively

All components of vectors and tensors will be taken with respect to a fixed orthonormal basis $\{\mathbf{e}_1, \mathbf{e}_2\}$ so that in particular, (ξ_1, ξ_2) are the coordinates of a generic particle in the reference configuration. The region occupied by the body in the reference configuration at time t is the half-plane

$$\mathcal{R}_{\rm R}(t) = \{(\xi_1, \xi_2) \,:\, \xi_2 < Z(t),\ -\infty < \xi_1 < \infty\}, \tag{14}$$

so that its boundary $\mathcal{S}_{\rm R}(t)$ is the horizontal straight line $\xi_2 = Z(t)$ as shown in Fig. 2(a). The unit outward normal vector is $\mathbf{e}_2$ and the propagation speed of a point on $\mathcal{S}_{\rm R}(t)$ is $\dot{Z}\,\mathbf{e}_2$. Note that $Z(t)$ is one of the unknowns to be determined.

The body undergoes a homogeneous deformation that maps[2] $(\xi_1, \xi_2) \to (x_1, x_2)$:

$$x_1 = \lambda_1 \xi_1, \quad x_2 = \lambda_2 \xi_2, \tag{15}$$

the stretches λ_1 and λ_2 being positive and constant. We consider λ_1 to be given. Therefore by (20) below, λ_2 is also known and constant. In the current configuration, the body occupies the half-plane

$$\mathcal{R}(t) = \{(x_1, x_2) \,:\, x_2 < X(t),\ -\infty < x_1 < \infty\}, \tag{16}$$

where

$$X(t) = \lambda_2 Z(t). \tag{17}$$

The boundary $\mathcal{S}(t)$ of the current configuration is the straight line $x_2 = X(t)$ as shown in Fig. 2(b). The unit outward normal is $\mathbf{e}_2$ and the propagation velocity of $\mathcal{S}(t)$ is $\dot{X}\,\mathbf{e}_2$. At the initial instant, we assume

$$X(0) = Z(0) = 0. \tag{18}$$

The deformation gradient tensor associated with (15) has components

$$[F] = \begin{pmatrix} \lambda_1 & 0 \\ 0 & \lambda_2 \end{pmatrix}, \tag{19}$$

[2] As stated previously, in general we use (y_1, y_2) to denote the coordinates of a particle in the current configuration. It is convenient however to use (x_1, x_2) in the special case of the homogeneous deformation.

and incompressibility, $\det \mathbf{F} = 1$, requires

$$\lambda_1 \lambda_2 = 1. \tag{20}$$

The components of the Piola and Cauchy stress tensors are found using (13) and (19) to be

$$[S] = \begin{pmatrix} G\lambda_1 - q_0(t)\lambda_1^{-1} & 0 \\ 0 & G\lambda_2 - q_0(t)\lambda_2^{-1} \end{pmatrix},$$
$$[T] = \begin{pmatrix} G\lambda_1^2 - q_0(t) & 0 \\ 0 & G\lambda_2^2 - q_0(t) \end{pmatrix}, \tag{21}$$

where, as mentioned above, $q_0(t)$ is the reactive pressure.

The boundary condition $(7)_2$ in the present context reads $\dot{p}_0(t) = \kappa \dot{X}(t)$. Integrating this with respect to t, using the initial condition $X(0) = 0$, and assuming the boundary to be traction-free at the initial instant, leads to

$$p_0(t) = \kappa X(t) \tag{22}$$

as expected. The boundary condition $(7)_1$ with $(21)_2$ gives

$$q_0(t) = G\lambda_2^2 + p_0(t) \overset{(22)}{=} G\lambda_2^2 + \kappa X(t) \overset{(17)}{=} G\lambda_2^2 + \kappa \lambda_2 Z(t), \tag{23}$$

where the surface tension plays no role since the curvature of the straight boundary is zero and we are limiting attention to the case where σ is constant. Keep in mind that q_0 is the reactive pressure entering through the constitutive relation while p_0 is the pressure on the boundary of the body.

From (3), (12), (19), $(21)_1$ and (23) we find the driving force to be

$$f_0(t) = \Delta\mu - \frac{G}{2}\left(\lambda_1 - \lambda_2\right)^2 - \kappa \lambda_2 Z(t), \tag{24}$$

and in view of the initial condition (18),

$$f_0(0) = \Delta\mu \; - \; (G/2)\left(\lambda_1 - \lambda_2\right)^2. \tag{25}$$

Note from (24) that as the boundary moves outwards, i.e., as Z increases, the driving force decreases and vice versa.

The kinetic relation (4) can be written using $V_R = \dot{Z}$ and (24) as the first order ordinary differential equation

$$\dot{f_0} = -\kappa \lambda_2 \mathsf{V}(f_0). \tag{26}$$

Figure 3 shows the f_0, $\dot{f_0}$-phase plane for (26). The trajectory passes through the origin and has the monotonicity shown in the figure because of the properties (5) of the kinetic response function V. It is seen from the phase plane that in the case $f_0(0) > 0$ (resp. $f_0(0) < 0$) the driving force decreases (resp. increases) monotonically from its initial value to the value 0. Since $\mathsf{V}(0) = 0$, growth stalls when $f_0(t) \to 0$. The phase plane shows that all motions are attracted to the equilibrium point $(0, 0)$, and so, within the context of the present section, are stable.

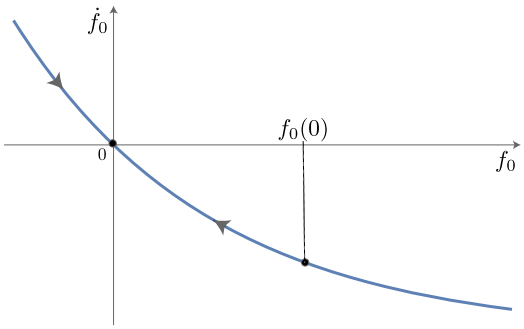

Fig. 3 Schematic phase plane for the first-order ordinary differential equation (26). The monotonicity of the curve shown follows from the properties of V in (5); the curvature may be different to what is shown but that has no effect on the results

In fact, one can integrate (26) to obtain[3]

$$\kappa t/\lambda_1 = \int_{f_0(t)}^{f_0(0)} \frac{1}{\mathsf{V}(f)}\, df. \tag{27}$$

This, together with (24) and (25), provides an algebraic equation that gives t as a function of Z. It can be readily verified that the right-hand side of (27) is a monotonically increasing function of Z and so this algebraic relation is uniquely invertible to give $Z(t)$. Moreover, if

$$\mathsf{V}(f) = \mathrm{O}(f^m) \quad \text{as} \quad f \to 0 \quad \text{where} \quad m \geq 1,$$

the integral in (27) tends to infinity as the lower limit tends to zero, implying that it takes infinite time for $f_0(t)$ to approach zero. For example in the special case of linear kinetics, $\mathsf{V}(f) = f/b$ where $b > 0$ is a constant parameter, (27) leads to the explicit expressions

$$f_0(t) = f_0(0)\, \mathrm{e}^{-\kappa t/(b\lambda_1)}, \quad Z(t) = \frac{\Delta\mu - (G/2)\big(\lambda_1 - \lambda_1^{-1}\big)^2}{\kappa/\lambda_1}\big[1 - \mathrm{e}^{-\kappa t/(b\lambda_1)}\big],$$

where we used (24) and (25) in getting to the second equation. Thus, as $t \to \infty$, we see that $\dot{Z} \to 0$ and so, eventually, the boundary stops moving and growth stalls.

In summary, once $Z(t)$ is determined from (27), the region $\mathcal{R}_{\mathrm{R}}(t)$ in the reference configuration is known from (14). Moreover, $X(t)$ is then given by (17), $p_0(t)$ by (22) and $q_0(t)$ by (23). All other quantities can then be calculated, both their time evolution and their limiting values as $t \to \infty$. The limiting solution is in equilibrium.

4 Perturbed Configuration. Linearized Problem

In order to investigate the stability of the time-dependent spatially homogeneous growth process, i.e., the homogeneous solution, found in Sect. 3, we now consider a perturbation of that solution. This involves perturbing *both* the deformation *and* the reference configuration. We start by linearizing the various equations about the homogeneous solution. The linearized field equations will therefore hold on the region $x_2 < X(t)$, $-\infty < x_1 < \infty$, see (16), and the boundary conditions will be enforced on the straight line $x_2 = X(t)$. We will use the symbol $\doteq$ in an equation to imply that quadratic and smaller terms have been neglected. The solution of the linearized problem will be examined in Sect. 5.

[3] We will frequently, without even a comment, use the incompressibility equation (20) to eliminate λ_2 in favor of λ_1^{-1} (or vice versa) as we have done here.

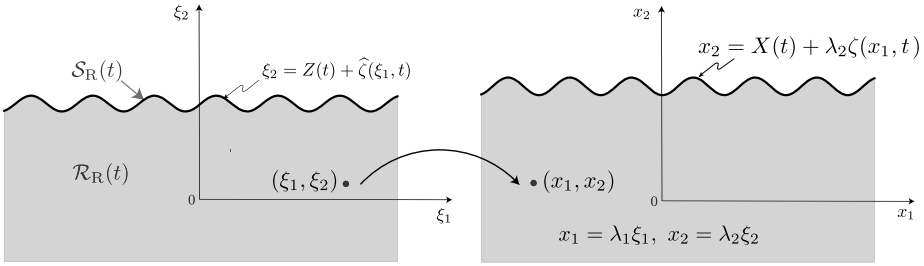

Fig. 4 Left: The perturbed reference configuration at time t is associated with the region $\mathcal{R}_{\rm R}(t)$: $\xi_2 < Z(t) + \widehat{\zeta}(\xi_1, t)$, $-\infty < \xi_1 < \infty$ whose boundary is $\mathcal{S}_{\rm R}(t)$. Right: The perturbed reference configuration mapped by $(\xi_1, \xi_2) \mapsto (x_1, x_2) = (\lambda_1 \xi_1, \lambda_2 \xi_2)$

Suppose that in the perturbed reference configuration, the body occupies the region

$$\mathcal{R}_{\rm R}(t) = \{(\xi_1, \xi_2) : \xi_2 < Z(t) + \widehat{\zeta}(\xi_1, t), \ -\infty < \xi_1 < \infty\}$$

at time t, as depicted in the left-hand figure in Fig. 4. Its boundary is the curve

$$\mathcal{S}_{\rm R}(t) = \{(\xi_1, \xi_2) : \xi_2 = Z(t) + \widehat{\zeta}(\xi_1, t), \ -\infty < \xi_1 < \infty\}. \tag{28}$$

The perturbation $\widehat{\zeta}$ of the boundary is assumed to be small. If we introduce the function $g(\xi_1, \xi_2, t) \coloneqq Z(t) + \widehat{\zeta}(\xi_1, t) - \xi_2$, then the boundary is the zero level set of g and therefore the unit outward normal vector to $\mathcal{S}_{\rm R}(t)$ is

$$\mathbf{n}_R = -\frac{\operatorname{grad}_\xi g}{|\operatorname{grad}_\xi g|} \doteq -\frac{\partial \widehat{\zeta}}{\partial \xi_1}\mathbf{e}_1 + \mathbf{e}_2 = \mathbf{e}_2 - \lambda_1 \frac{\partial \zeta}{\partial x_1}\mathbf{e}_1, \tag{29}$$

where in the last step we have introduced

$$\zeta(x_1, t) \coloneqq \widehat{\zeta}(\xi_1, t) \quad \text{with} \quad x_1 = \lambda_1 \xi_1. \tag{30}$$

The propagation speed $V_R = \mathbf{V}_R \cdot \mathbf{n}_R$ of $\mathcal{S}_{\rm R}(t)$ is

$$V_R = -\frac{\dot{g}}{|\operatorname{grad}_\xi g|} \doteq \dot{Z} + \dot{\zeta} \quad \text{where} \quad \dot{\zeta} = \frac{\partial \zeta}{\partial t}(x_1, t) = \frac{\partial \widehat{\zeta}}{\partial t}(\xi_1, t). \tag{31}$$

We now perturb the deformation studied in Sect. 3 so that at each instant t, $(\xi_1, \xi_2) \to (y_1, y_2)$ according to

$$y_1 = x_1 + u_1(x_1, x_2, t), \quad y_2 = x_2 + u_2(x_1, x_2, t), \tag{32}$$

where $x_1 = \lambda_1 \xi_1$, $x_2 = \lambda_2 \xi_2$. The displacement components u_1, u_2 and their derivatives are assumed to be small.

The boundary $\mathcal{S}(t)$ of the body in the current configuration can be determined by setting $x_2 = X(t) + \lambda_2 \zeta(x_1, t)$ in (32) and linearizing. This leads to the following parametric characterization of $\mathcal{S}(t)$:

$$\left.\begin{aligned} y_1 &= \overline{y}_1(x_1, t) \doteq x_1 + u_1(x_1, X(t), t), \\ y_2 &= \overline{y}_2(x_1, t) \doteq X(t) + \lambda_2 \zeta(x_1, t) + u_2(x_1, X(t), t), \end{aligned}\right\} \tag{33}$$

where $x_1 \in (-\infty, \infty)$ is the parameter and $X(t) = \lambda_2 Z(t)$. The unit outward normal vector on $\mathcal{S}(t)$ is

$$\mathbf{n} = \frac{-\overline{y}_{2,1}\mathbf{e}_1 + \overline{y}_{1,1}\mathbf{e}_2}{\sqrt{(\overline{y}_{1,1})^2 + (\overline{y}_{2,1})^2}} \doteq \mathbf{e}_2 - (\lambda_2\zeta_{,1} + u_{2,1})\mathbf{e}_1, \tag{34}$$

where here, and henceforth, we use the notation

$$h_{,i} := \frac{\partial h}{\partial x_i}, \quad i = 1, 2,$$

for any function $h(x_1, x_2, t)$. We also need to calculate the curvature, $\varkappa$, of the curve $\mathcal{S}(t)$ for which we use the formula[4]

$$\varkappa = \frac{\overline{y}_{1,1}\overline{y}_{2,11} - \overline{y}_{2,1}\overline{y}_{1,11}}{\left[\left(\overline{y}_{1,1}\right)^2 + \left(\overline{y}_{2,1}\right)^2\right]^{3/2}}. \tag{35}$$

Substituting (33) into (35) and linearizing leads to

$$\varkappa \doteq \lambda_2\zeta_{,11} + u_{2,11}. \tag{36}$$

4.1 Field Equations

The deformation gradient tensor $\mathbf{F} = \text{grad}_\xi \mathbf{y}$ associated with the perturbed deformation (32) has components

$$[F] = \begin{pmatrix} \lambda_1 + \lambda_1 u_{1,1} & \lambda_2 u_{1,2} \\ \lambda_1 u_{2,1} & \lambda_2 + \lambda_2 u_{2,2} \end{pmatrix}. \tag{37}$$

Incompressibility, $\det[F] = 1$, requires $\lambda_1\lambda_2 = 1$ and

$$u_{1,1} + u_{2,2} = 0. \tag{38}$$

Since

$$[F]^{-1} \doteq \begin{pmatrix} \lambda_2 + \lambda_2 u_{2,2} & -\lambda_2 u_{1,2} \\ -\lambda_1 u_{2,1} & \lambda_1 + \lambda_1 u_{1,1} \end{pmatrix}, \tag{39}$$

the Piola stress $\mathbf{S} = G\mathbf{F} - q\mathbf{F}^{-T}$ can be written as

$$[S] \doteq \begin{pmatrix} [G\lambda_1 - q_0\lambda_2] + G\lambda_1 u_{1,1} - q_0\lambda_2 u_{2,2} - \lambda_2\tilde{q} & G\lambda_2 u_{1,2} + q_0\lambda_1 u_{2,1} \\ G\lambda_1 u_{2,1} + q_0\lambda_2 u_{1,2} & [G\lambda_2 - q_0\lambda_1] + G\lambda_2 u_{2,2} - q_0\lambda_1 u_{1,1} - \lambda_1\tilde{q} \end{pmatrix}, \tag{40}$$

where we have expressed the reactive pressure as

$$q = q_0 + \tilde{q}.$$

[4] See equation (A.10) in Appendix A.

The perturbation $\tilde{q}$ is assumed to be small. The Cauchy stress $\mathbf{T} = \mathbf{S}\mathbf{F}^T$ is

$$[T] \doteq \begin{pmatrix} [G\lambda_1^2 - q_0] + 2G\lambda_1^2 u_{1,1} - \widetilde{q} & G(\lambda_1^2 u_{2,1} + \lambda_2^2 u_{1,2}) \\ G(\lambda_1^2 u_{2,1} + \lambda_2^2 u_{1,2}) & [G\lambda_2^2 - q_0] + 2G\lambda_2^2 u_{2,2} - \widetilde{q} \end{pmatrix}. \tag{41}$$

The equilibrium equation $(9)_2$ can be approximated as $T_{11,1} + T_{12,2} \doteq 0$ and $T_{21,1} + T_{22,2} \doteq 0$. Substituting (41) into this yields

$$\tilde{q}_{,1} = G\,(\lambda_1^2 u_{1,11} + \lambda_2^2 u_{1,22}), \quad \tilde{q}_{,2} = G\,(\lambda_1^2 u_{2,11} + \lambda_2^2 u_{2,22}). \tag{42}$$

We will frequently use the incompressibility equation (38), often without explicitly saying so, to replace $u_{2,2}$ by $-u_{1,1}$ (or vice versa) as we have done here.

4.2 Boundary Conditions

Kinetic relation: Now consider the driving force (3) associated with growth. On substituting the expressions (12), (29), (37) and (40) for W, $\mathbf{n}_\mathrm{R}$, $\mathbf{F}$ and $\mathbf{S}$ into $f = \Delta\mu + \mathbf{S}\mathbf{n}_R \cdot \mathbf{F}\mathbf{n}_R - W(\mathbf{F})$ and linearizing, one obtains

$$f \doteq f_0 - G(\lambda_1^2 + \lambda_2^2)u_{1,1} - \widetilde{q}, \tag{43}$$

where f_0 is the driving force in the unperturbed problem given in (24). When the expressions (31) and (43), for the propagation speed V_R and the driving force f are used in the kinetic relation $V_R = \mathsf{V}(f)$, linearization leads to $\dot{Z} = \mathsf{V}(f_0)$ and

$$b\dot{\zeta} = -G(\lambda_1^2 + \lambda_2^2)u_{1,1} - \widetilde{q}, \tag{44}$$

where we have set

$$b := 1/\mathsf{V}'(f_0) > 0. \tag{45}$$

Note that $f_0 = f_0(t)$ during the evolution of the homogeneous solution and so $b = b(t)$ is also a function of time.

Mechanical boundary condition: An expression for the unit normal vector $\mathbf{n}$ was determined previously in (34). Therefore on using (41) and $p = p_0 + \widetilde{p}$, the boundary condition[5] $\mathbf{T}\mathbf{n} = -p\mathbf{n} + \sigma\varkappa\mathbf{n}$ approximates to

$$u_{1,2} + u_{2,1} = \lambda_1(\lambda_1^2 - \lambda_2^2)\zeta_{,1}, \quad 2G\lambda_2^2 u_{1,1} + \widetilde{q} = \widetilde{p} - \sigma\varkappa; \tag{46}$$

where, from (36), the curvature is $\varkappa = \lambda_2\zeta_{,11} + u_{2,11}$.

The second part of the mechanical boundary condition, $(7)_2$, requires that we enforce $\dot{p} = \kappa\mathbf{V}\cdot\mathbf{n}$. Recalling from (1) that $\mathbf{V} = \mathbf{F}\mathbf{V}_R + \mathbf{v}$, we can now use the previously determined expressions for $\mathbf{n}_\mathrm{R}$, $\mathbf{V}_\mathrm{R}$, $\mathbf{n}$ and $\mathbf{F}$ from (29), (31), (34) and (37) to calculate

$$\mathbf{V}\cdot\mathbf{n} = \mathbf{F}\mathbf{V}_R\cdot\mathbf{n} + \mathbf{v}\cdot\mathbf{n} \doteq \dot{X} + \lambda_2\dot{\zeta} + \dot{X}u_{2,2} + \dot{u}_2,$$

[5] Recall that the third term on the right-hand side of $(7)_1$ is absent since we are concerned with the case where σ is constant.

having also used $\mathbf{v} = \dot{u}_1\mathbf{e}_1 + \dot{u}_2\mathbf{e}_2$. Therefore $\dot{p} = \kappa\mathbf{V}\cdot\mathbf{n}$ gives $\dot{p}_0 = \kappa\dot{X}$ and

$$\dot{\widetilde{p}} = \kappa\Big(\lambda_2\dot{\zeta} + \dot{X}u_{2,2} + \dot{u}_2\Big) = \kappa\left(\lambda_2\dot{\zeta} + \frac{d}{dt}u_2(x_1, X(t), t)\right).$$

Integrating this with respect to time gives

$$\widetilde{p} = \kappa(\lambda_2\zeta + u_2), \tag{47}$$

where we have taken the perturbation of the pressure to vanish when the boundary and displacement perturbations vanish, i.e., $\widetilde{p} = 0$ when $\zeta = 0$, $u_2 = 0$. The term in parenthesis on the right-hand side of (47) is precisely the vertical displacement increment $\overline{y}_2(x_1, t) - X(t)$ of the boundary $\mathcal{S}(t)$ as one might expect; see (33).

4.3 Summary

The perturbed fields $u_1(x_1, x_2, t)$, $u_2(x_1, x_2, t)$ and $\widetilde{q}(x_1, x_2, t)$ obey the field equations (38) and $(42)_{1,2}$. They hold on $x_2 < X(t)$, $-\infty < x_1 < \infty$. The associated boundary conditions are (44), $(46)_{1,2}$ and (47), and they involve the additional fields $\widetilde{p}(x_1, t)$, $\zeta(x_1, t)$ as well. The boundary conditions hold on $x_2 = X(t)$, $-\infty < x_1 < \infty$.

It is convenient to eliminate $\widetilde{q}$ and $\widetilde{p}$ from the problem. First, $\widetilde{q}$ can be eliminated from the field equations by differentiating $(42)_1$ with respect to x_2, $(42)_2$ with respect to x_1 and equating the results. Turning to the boundary conditions, we use (47) to eliminate $\widetilde{p}$ from $(46)_2$, then differentiate the result with respect to x_1 and use $(42)_1$ to eliminate $\widetilde{q}_{,1}$. Finally, we eliminate $\widetilde{q}$ from (44) by using $(46)_2$ and (47).

This leads[6] to the following mathematical problem for the displacement and boundary perturbation fields, $u_1(x_1, x_2, t)$, $u_2(x_1, x_2, t)$ and $\zeta(x_1, t)$:

$$\left.\begin{aligned} u_{1,1} + u_{2,2} &= 0,\\ -\lambda_1^2 u_{2,111} + (\lambda_1^2 + \lambda_2^2)u_{1,112} + \lambda_2^2 u_{1,222} &= 0,\end{aligned}\right\} \quad \text{for} \quad x_2 < X(t),\ -\infty < x_1 < \infty, \tag{48}$$

$$\left.\begin{aligned} u_{1,2} + u_{2,1} &= \lambda_1(\lambda_1^2 - \lambda_2^2)\zeta_{,1},\\ \kappa\lambda_2\zeta_{,1} - \sigma\lambda_2\zeta_{,111} &= G(\lambda_1^2 + 2\lambda_2^2)u_{1,11} + G\lambda_2^2 u_{1,22} - \kappa u_{2,1} + \sigma u_{2,111},\\ b\dot{\zeta} + \kappa\lambda_2\zeta - \sigma\lambda_2\zeta_{,11} &= -G(\lambda_1^2 - \lambda_2^2)u_{1,1} - \kappa u_2 + \sigma u_{2,11},\end{aligned}\right\}$$
$$\text{on} \quad x_2 = X(t). \tag{49}$$

5 Solution of the Linearized Problem

The general solution of $(48)_1$ is

$$u_1 = \psi_{,2}\,, \quad u_2 = -\psi_{,1}\,, \tag{50}$$

[6] In these calculations, and elsewhere, we shall often simplify algebraic expressions using the incompressibility conditions $\lambda_1\lambda_2 = 1$ and $u_{2,2} = -u_{1,1}$ when convenient.

for any function $\psi(x_1, x_2, t)$. The remaining field equation $(48)_2$ can now be written as

$$\lambda_1^2\psi_{,1111} + (\lambda_1^2 + \lambda_2^2)\psi_{,1122} + \lambda_2^2\psi_{,2222} = 0 \quad \text{for} \quad -\infty < x_1 < \infty,\ x_2 < X(t). \tag{51}$$

On substituting (50) into the boundary conditions (49) we get

$$\left.\begin{aligned} \psi_{,22} - \psi_{,11} &= \lambda_1(\lambda_1^2 - \lambda_2^2)\zeta_{,1}, \\ \kappa\lambda_2\zeta_{,1} - \sigma\lambda_2\zeta_{,111} &= G(\lambda_1^2 + 2\lambda_2^2)\psi_{,112} + G\lambda_2^2\psi_{,222} + \kappa\psi_{,11} - \sigma\psi_{,1111}, \\ b(t)\dot{\zeta} + \kappa\lambda_2\zeta - \sigma\lambda_2\zeta_{,11} &= -G(\lambda_1^2 - \lambda_2^2)\psi_{,12} + \kappa\psi_{,1} - \sigma\psi_{,111}, \end{aligned}\right\}$$
$$\text{on } x_2 = X. \tag{52}$$

The problem has now been reduced to finding $\psi(x_1, x_2, t)$ and $\zeta(x_1, t)$.

Keeping in mind that the coefficient $b(t)$ in $(52)_3$ is time-dependent, we seek a solution in the separable form

$$\psi(x_1, x_2, t) = \mathrm{e}^{ikx_1}h(y)C(t), \quad \zeta(x_1, t) = \mathrm{e}^{ikx_1}Q(t), \tag{53}$$

where

$$y := k(x_2 - X(t)). \tag{54}$$

Substituting $(53)_1$ into (51) yields the ordinary differential equation

$$h''''(y) - (\lambda_1^4 + 1)h''(y) + \lambda_1^4 h(y) = 0, \quad y < 0, \tag{55}$$

whose solution that is bounded for $y \to -\infty$ is

$$h(y) = \alpha\,\mathrm{e}^{y} + \beta\,\mathrm{e}^{\lambda_1^2 y}; \tag{56}$$

here, α and β are constants to be determined, and with no loss of generality we have assumed $k > 0$.

Substituting (53) into the boundary conditions (52) leads to

$$ik[h''(0) + h(0)]C(t) = -\lambda_1(\lambda_1^2 - \lambda_2^2)Q(t), \tag{57}$$

$$i(\kappa + \sigma k^2)\lambda_2 Q(t) = \Big[k^2 G\big[\lambda_2^2 h'''(0) - (\lambda_1^2 + 2\lambda_2^2)h'(0)\big] - (\kappa + \sigma k^2)kh(0)\Big]C(t), \tag{58}$$

$$b(t)\dot{Q}(t) + (\kappa + \sigma k^2)\lambda_2 Q(t) = ik\Big[- kG(\lambda_1^2 - \lambda_2^2)h'(0) + (\kappa + \sigma k^2)h(0)\Big]C(t). \tag{59}$$

Equations (57) and (58) both imply that $C(t)/Q(t)$ is time-independent. Thus, let

$$Q(t) = ik\gamma C(t), \tag{60}$$

where γ is a constant to be determined. Substituting (60) into (57)-(59) gives

$$h''(0) + h(0) + \gamma\lambda_1(\lambda_1^2 - \lambda_2^2) = 0, \tag{61}$$

$$Gk\lambda_2^2 h'''(0) - Gk(\lambda_1^2 + 2\lambda_2^2)h'(0) - (\kappa + \sigma k^2)h(0) + (\kappa + \sigma k^2)\lambda_2\gamma = 0, \tag{62}$$

$$\gamma\, b(t)\dot{C}(t) + \Big[Gk(\lambda_1^2 - \lambda_2^2)h'(0) - (\kappa + \sigma k^2)h(0) + (\kappa + \sigma k^2)\lambda_2\gamma\Big]C(t) = 0. \tag{63}$$

In writing (63) (and (59) above) we have explicitly reminded ourselves that in general, b is time-dependent: $b = b(t) = 1/\mathsf{V}'(f_0(t))$; see (45) and (26). Equation (63) tells us that $b(t)\dot{C}(t)/C(t)$ is time-independent, and so we can write

$$b(t)\dot{C}(t)/C(t) = \nu, \tag{64}$$

where the constant ν is to be determined. Substituting (64) into (63) yields

$$Gk(\lambda_1^2 - \lambda_2^2)h'(0) - (\kappa + \sigma k^2)h(0) + [(\kappa + \sigma k^2)\lambda_2 + \nu]\gamma = 0. \tag{65}$$

The 4 unknown parameters α, β, γ and ν are to be determined from (56), (61), (62) and (65).

The time evolution of the perturbation is governed by (64). In the special case where the homogeneous solution is in equilibrium, the associated driving force vanishes, i.e., $f_0(t) = 0$ for all time, and so $b(t)$ is constant. Then (64) yields

$$C(t) = \mathrm{e}^{\nu t/b} \tag{66}$$

(to within a multiplicative constant). Therefore perturbations decay with time provided $\nu < 0$. When the homogeneous solution is not in equilibrium, equation (64) leads to

$$\frac{1}{C}\frac{dC}{dt} = \frac{\nu}{b(t)} \overset{(45)}{=} \nu\mathsf{V}'(f_0) = \frac{\nu}{\dot{f}_0}\frac{d}{dt}\mathsf{V}(f_0) \overset{(26)}{=} -\frac{\nu\lambda_1}{\kappa}\frac{1}{\mathsf{V}(f_0)}\frac{d}{dt}\mathsf{V}(f_0)$$

and therefore, (again to within a multiplicative constant),

$$C(t) = \left[\frac{1}{|\mathsf{V}(f_0(t))|}\right]^{\nu\lambda_1/\kappa}.$$

Recall from the discussion surrounding the phase plane in Figure (3) that $\mathsf{V}(f_0(t))$ approaches zero as $t \to \infty$, and so again, $C(t)$ (and therefore perturbations) decay when $\nu < 0$.

Our goal is to study the sign of ν where stability demands $\nu < 0$ for all perturbations. In principle, ν can be a function of, at most, λ_1, G, κ, σ and k. However, observe that the stiffness κ and the surface tension σ do not appear in (61), and they enter as a pair, $\kappa + \sigma k^2$, in (62) and (65). Thus ν can in fact be expressed as a function of λ_1, Gk and $\kappa + \sigma k^2$. The Pi theorem of dimensional analysis can now be used to infer that

$$N = \widehat{\nu}\,(\lambda_1, K) \quad \text{where} \quad N := \frac{\nu}{Gk}, \quad K := \frac{\kappa + \sigma k^2}{Gk}. \tag{67}$$

Once the expression (56) for $h(y)$ is substituted into (61), (62) and (65), we have a system of 3 homogeneous linear algebraic equations for α, β and γ that we can write as:

$$\begin{pmatrix} 2 & \lambda_1^4 + 1 & \lambda_1(\lambda_1^2 - \lambda_2^2) \\ (1 + \lambda_1^4) + \lambda_1^2 K & (2 + K)\lambda_1^2 & -\lambda_1 K \\ (\lambda_1^2 - \lambda_2^2) - K & (\lambda_1^4 - 1) - K & \lambda_2 K + N \end{pmatrix} \begin{pmatrix} \alpha \\ \beta \\ \gamma \end{pmatrix} = \begin{pmatrix} 0 \\ 0 \\ 0 \end{pmatrix}.$$

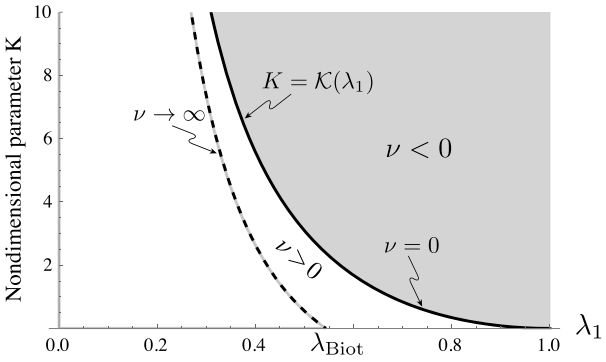

Fig. 5 Perturbations decay at points in the shaded region $K > \mathcal{K}(\lambda_1)$

Necessary and sufficient for this system to have a nontrivial solution $\{\alpha, \beta, \gamma\}$ is that the determinant of the coefficient matrix vanish. This leads to an algebraic equation that is linear in N. Solving for N gives

$$N = \frac{\nu}{Gk} = \frac{(\lambda_1^2+1)(1-\lambda_1^4)^2 - \lambda_1^2(1+\lambda_1^2+3\lambda_1^4-\lambda_1^6)\,K}{\lambda_1[(\lambda_1^6+\lambda_1^4+3\lambda_1^2-1)+\lambda_1^2(\lambda_1^2+1)\,K]}. \tag{68}$$

We now examine the sign of ν on the λ_1, K-plane where, because our interest is in compression, we restrict attention to $0 < \lambda_1 \le 1$. (In Appendix C we extend the results to the case of extensional stretches.) First, observe that the numerator of (68) vanishes on the curve

$$K = \mathcal{K}(\lambda_1), \quad 0 < \lambda_1 \le 1, \tag{69}$$

where

$$\mathcal{K}(\lambda) := \frac{(\lambda^2+1)(1-\lambda^4)^2}{\lambda^2(1+\lambda^2+3\lambda^4-\lambda^6)}, \quad 0 < \lambda \le 1. \tag{70}$$

This corresponds to the thick solid curve in Fig. 5 which is monotonic, with $\mathcal{K}(\lambda_1) \to \infty$ as $\lambda_1 \to 0^+$. Second, one finds that ν given by (68) is negative in the shaded region above this curve:

$$\nu < 0 \quad \text{for} \quad K > \mathcal{K}(\lambda_1), \quad 0 < \lambda_1 \le 1. \tag{71}$$

There is another region of this plane on which $\nu < 0$ corresponding to the left-hand side of the dashed curve in Fig. 5. The dashed curve corresponds to the vanishing of the denominator of (68) and so ν is unbounded on it. This region involves compression that is more severe than that associated with the gray region. *Thus we shall not consider it from here on.*

Accordingly, consider points (λ_1, K) in the interior of the gray region of the λ_1, K-plane shown in Fig. 5. Since $\nu < 0$ in this region, perturbations associated with this region decay with time. In general, the homogeneous solution corresponding to some value of $\lambda_1 \in (0, 1)$, is stable for sufficiently large values of K, specifically for $K > \mathcal{K}(\lambda_1)$. Observe from the figure that the particular steady solution corresponding to $\lambda_1 = 1$ is stable for all $K > 0$.

It is important to emphasize that K defined in $(67)_3$ is not a simple scaling of the wave number. It is illuminating to write K as

$$K = \frac{\kappa}{Gk} + \frac{\sigma k}{G}, \tag{72}$$

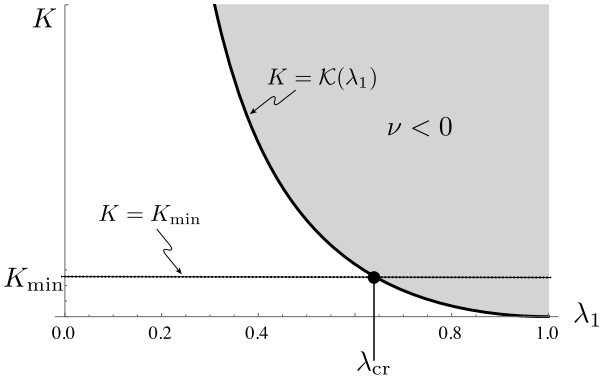

Fig. 6 The homogeneous solution corresponding to a value of $\lambda_1 \in (\lambda_{cr}, 1)$ is stable for *all* wave numbers k. The critical value of the stretch λ_{cr} at instability is given by (75) where $\overline{\ell} = \sigma\kappa/G^2$

in which one term involves the wave number k nondimensionalized with the length-scale σ/G, and the other term involves the reciprocal of the wave number nondimensionalized with the length-scale G/κ. Consider the special case where the compliant ambient medium is absent: $\kappa = 0$. Then $K \propto k$ and so we conclude from the previous paragraph that the homogeneous solution is stable for sufficiently *large* wave numbers k. On the other hand, in the special case without surface tension, $\sigma = 0$, we have $K \propto 1/k$. Thus in this case we conclude that the homogeneous solution is stable for sufficiently *small* wave numbers k. Thus we see that κ and σ work in complementary ways.

In order to study the sign of ν for various wave numbers k, observe that K is strictly positive and that its smallest value (as a function of k) is

$$K_{\min} = 2\big(\overline{\ell}\big)^{1/2}, \tag{73}$$

where the non-dimensional parameter

$$\overline{\ell} := \frac{\sigma\kappa}{G^2} \tag{74}$$

is the ratio of the two length-scales G/κ and σ/G. The wave number at which K takes its minimum value is $k = k_{cr} := \sqrt{\kappa/\sigma}$. Figure 6 shows Fig. 5 again but now with the line $K = K_{\min}$ added to it. Let λ_{cr} be the value of stretch at which the bold solid curve $K = \mathcal{K}(\lambda_1)$ intersects the horizontal line $K = K_{\min}$. This critical value of stretch is given by the unique root in (0, 1) of the equation

$$2\big(\overline{\ell}\big)^{1/2} = \mathcal{K}(\lambda_{cr}). \tag{75}$$

Collecting the preceding results, we know from $(71)_2$ and (72) that the homogeneous solution associated with a stretch λ_1 is stable against a perturbation with wave number k if $\kappa/(Gk) + \sigma k/G > \mathcal{K}(\lambda_1)$. Therefore it is stable against perturbations of all wave numbers provided the smallest value of $\kappa/(Gk) + \sigma k/G$ over all $k > 0$ exceeds $\mathcal{K}(\lambda_1)$, i.e., provided $K_{\min} > \mathcal{K}(\lambda_1)$. From (73) and (75) this requires $\mathcal{K}(\lambda_{cr}) > \mathcal{K}(\lambda_1)$ which, by the monotonicity of $\mathcal{K}(\lambda)$, is equivalent to $\lambda_{cr} < \lambda_1 \le 1$; see Fig. 6. We thus conclude that $\nu < 0$ for *all wave numbers* k provided $\lambda_{cr} < \lambda_1 \le 1$ and therefore that the threshold for instability is $\lambda_1 = \lambda_{cr}$. The corresponding critical wave number is $k_{cr} = \sqrt{\kappa/\sigma}$ introduced below (74).

Observe that as $\overline{\ell} = \sigma\kappa/G^2$ increases, (73) tells us that $K_{\min}$ increases, and so from Fig. 6 we conclude that λ_{cr} decreases. In fact, $\lambda_{cr} \to 1$ as $\overline{\ell} \to 0$ and $\lambda_{cr} \to 0^+$ as $\overline{\ell} \to \infty$.

Stated differently, suppose the ambient environment offers no resistance to growth. Then, the stiffness $\kappa \to 0$ and so $\overline{\ell} \to 0$ according to $(74)_2$ and $K_{\min} \to 0$ by (73). Then we see from Fig. 6 that $\lambda_{\rm cr} \to 1$. Thus the only homogeneous solution that is stable against all perturbation is the one with $\lambda_1 = 1$. On the other hand if the ambient environment is rigid, then $\kappa \to \infty$, $\overline{\ell} \to \infty$ and $K_{\min} \to \infty$ and so $\lambda_{\rm cr} \to 0^+$. Thus all homogeneous solutions are stable in this case. The results of these two special cases coincide with what was found in [4].

Finally, we remark that $\lambda_{\rm cr}$ need not exceed $\lambda_{\rm Biot}$. By substituting $\lambda_{\rm cr} = \lambda_{\rm Biot}$ into $(75)_1$ we find that $\lambda_{\rm cr} = \lambda_{\rm Biot}$ when $\overline{\ell} \approx 1.4196$. For $\overline{\ell}$ greater than this value $\lambda_{\rm cr} < \lambda_{\rm Biot}$ and vice versa.

Appendix A: Some Results Concerning an Evolving Curve in the Plane

For a more general treatment of the material in this appendix, see Gurtin [21].

Let $\mathcal{S}(t)$ be a curve in the y_1, y_2-plane, described parametrically by

$$\mathbf{y}(p,t) = y_1(p,t)\mathbf{e}_1 + y_2(p,t)\mathbf{e}_2, \quad p_1 \le p \le p_2, \tag{A.1}$$

p being the parameter, t time and $\{\mathbf{e}_1, \mathbf{e}_2\}$ a fixed orthonormal basis. For any function $h(p,t)$ we let a prime and dot denote

$$h' = \frac{\partial h}{\partial p}(p,t), \quad \dot{h} = \frac{\partial h}{\partial t}(p,t), \tag{A.2}$$

respectively. Let

$$\lambda = \sqrt{\left(y_1'\right)^2 + \left(y_2'\right)^2} \tag{A.3}$$

denote the stretch along $\mathcal{S}$. The arc length $s(p,t)$ is found by integrating

$$s' = \lambda \tag{A.4}$$

with respect to p. The unit tangent vector on $\mathcal{S}$ (in the direction of increasing arc length) is

$$\mathbf{t} = \cos\theta\, \mathbf{e}_1 + \sin\theta\, \mathbf{e}_2, \tag{A.5}$$

where the angle $\theta(p,t)$ that the tangent makes with the y_1-axis is given by

$$\cos\theta = y_1'/\lambda, \quad \sin\theta = y_2'/\lambda. \tag{A.6}$$

The unit normal vector, obtained by counter clockwise rotation of $\mathbf{t}$, is

$$\mathbf{n} = -\sin\theta\, \mathbf{e}_1 + \cos\theta\, \mathbf{e}_2. \tag{A.7}$$

The curvature of $\mathcal{S}$, by definition, is

$$\varkappa := \frac{\partial \theta}{\partial s} = \theta'/\lambda, \tag{A.8}$$

having used (A.4). It follows from (A.5), (A.7) and (A.8) that

$$\mathbf{n}' = -\varkappa\lambda\mathbf{t}, \quad \mathbf{t}' = \varkappa\lambda\mathbf{n}. \tag{A.9}$$

Differentiating each equation in (A.6) with respect to p leads to the respective equations

$$-\sin\theta\,\theta' = y_1''/\lambda - \cos\theta\lambda'/\lambda, \quad \cos\theta\,\theta' = y_2''/\lambda - \sin\theta\lambda'/\lambda.$$

Multiplying the first of these by $\sin\theta$, the second by $\cos\theta$ and then subtracting the first from the second gives

$$\theta' = \cos\theta\, y_2''/\lambda - \sin\theta\, y_1''/\lambda \overset{(A.6)}{=} (y_1'\, y_2'' - y_2'\, y_1'')/\lambda^2.$$

On combining this with (A.3) and (A.8), we obtain the following formula for the curvature:

$$\varkappa = \frac{y_1' y_2'' - y_2' y_1''}{\left[(y_1')^2 + (y_2')^2\right]^{3/2}}. \tag{A.10}$$

This was written down previously in (35).

The velocity of the point p of the evolving curve $\mathcal{S}(t)$ is

$$\mathbf{V} = \dot{\mathbf{y}} = \dot{y}_1\mathbf{e}_1 + \dot{y}_2\mathbf{e}_2. \tag{A.11}$$

Next, differentiating (A.3) with respect to t and using (A.5), (A.6) and (A.11) gives

$$\dot{\lambda} = (y_1'\dot{y}_1' + y_2'\dot{y}_2')/\lambda = \mathbf{t}\cdot\mathbf{V}'. \tag{A.12}$$

Let V and U be the normal and tangential components of $\mathbf{V}$:

$$\mathbf{V} = V\,\mathbf{n} + U\,\mathbf{t}. \tag{A.13}$$

Then

$$\begin{aligned}\dot{\lambda} &\overset{(A.12)}{=} \mathbf{t}\cdot\mathbf{V}' \overset{(A.13)}{=} \mathbf{t}\cdot(V'\,\mathbf{n} + V\,\mathbf{n}' + U'\,\mathbf{t} + U\mathbf{t}') \\ &\overset{(A.9)}{=} \mathbf{t}\cdot(-\varkappa\lambda V\,\mathbf{t} + U'\mathbf{t}) \overset{(A.4)}{=} -\varkappa\lambda V + \lambda\frac{\partial U}{\partial s}.\end{aligned} \tag{A.14}$$

Finally, let $w(\lambda)$ be a function defined for $\lambda > 0$. Then, the rate of change of the integral of $w(\lambda(s,t))$ over $\mathcal{S}(t)$ is

$$\begin{aligned}\frac{d}{dt}\int_{\mathcal{S}(t)} w\,ds &\overset{(A.4)}{=} \frac{d}{dt}\int_{p_1}^{p_2} w\lambda\,dp = \int_{p_1}^{p_2}(\dot{w}\lambda + w\dot{\lambda})\,dp = \int_{p_1}^{p_2}\left(\frac{dw}{d\lambda}\lambda + w\right)\dot{\lambda}\,dp = \\ &\overset{(A.4)}{=} \int_{\mathcal{S}(t)}\left(\frac{dw}{d\lambda}\lambda + w\right)\dot{\lambda}\lambda^{-1}\,ds \\ &\overset{(A.14)}{=} -\int_{\mathcal{S}(t)}\left(\frac{dw}{d\lambda}\lambda + w\right)\left(\varkappa V - \frac{\partial U}{\partial s}\right)ds.\end{aligned} \tag{A.15}$$

This will be used in Appendix B.

Appendix B: The Driving Force

The material in this appendix generalizes the calculation of Tomassetti et al. [35] to include both the pressure loading and surface tension. Even though we have taken the surface tension σ to be constant in Sects. 3 – 5 of the present paper, the analysis in this appendix is not limited to that case. For a more general treatment of surface energy, see Wu [36], Freund [17] and Fried and Gurtin [18].

The dissipation rate, $\mathbb{D}$, associated with the growing body is defined to be the difference between (i) the rate of mechanical working plus the rate of influx of chemical energy and (ii) the rate of increase of bulk and surface energy. Thus

$$\mathbb{D} := \int_{\mathcal{S}(t)} \mathbf{T}^{+}\mathbf{n}\cdot\mathbf{V}\,dA + \int_{\mathcal{S}_{\mathrm{R}}(t)} \Delta\mu\, V_{\mathrm{R}}\,dA_{\mathrm{R}} - \frac{d}{dt}\int_{\mathcal{R}_{\mathrm{R}}(t)} W\,d\mathcal{V}_{\mathrm{R}} - \frac{d}{dt}\int_{\mathcal{S}(t)} w\,dA, \tag{B.1}$$

where, since $\mathcal{S}(t)$ is a closed curve, the surface tension is an internal force and so does not contribute to the rate of working. Here, in the notation above equation (7), $\mathbf{T}^{+}\mathbf{n}$ is the mechanical traction on the boundary $\mathcal{S}(t)$ of the body in the current configuration, and $\mathbf{V}$ is its propagation velocity; $\Delta\mu$ is the difference in chemical energy per unit reference volume between material units unattached and attached to the body, and[7] $V_{\mathrm{R}} = \mathbf{V}_{\mathrm{R}}\cdot\mathbf{n}_{\mathrm{R}}$ is the normal propagation speed of the referential boundary; $W(\mathbf{F})$ is the bulk elastic energy per unit reference volume; and w is the surface energy per unit current area. For simplicity, we speak here of volumes and areas despite our setting being two dimensional (where one can imagine the body to have unit depth into the page). Finally, we take the surface energy to be $w = w(\lambda)$ where λ is the stretch along the boundary.

The rate of mechanical working term in (B.1) can be written, using the boundary condition (6) with $\mathbf{T}^{-} = \mathbf{T}$, as

$$\begin{aligned}\int_{\mathcal{S}(t)} \mathbf{T}^{+}\mathbf{n}\cdot\mathbf{V}\,dA &= \int_{\mathcal{S}(t)} \mathbf{T}\mathbf{n}\cdot\mathbf{V}\,dA - \int_{\mathcal{S}(t)} \left(\sigma\varkappa V + \frac{\partial\sigma}{\partial s}U\right) dA\\ &= \int_{\mathcal{S}(t)} \mathbf{T}\mathbf{n}\cdot\mathbf{V}\,dA - \int_{\mathcal{S}(t)} \sigma\left(\varkappa V - \frac{\partial U}{\partial s}\right) dA,\end{aligned} \tag{B.2}$$

where $\varkappa$ is the curvature of the boundary in the current configuration, $V = \mathbf{V}\cdot\mathbf{n}$, $U = \mathbf{V}\cdot\mathbf{t}$ and in getting to the last equality we have integrated $\frac{\partial\sigma}{\partial s}U$ by parts over the closed curve $\mathcal{S}$. The first term on the right-hand side of (B.2) can be dealt with in a standard manner using $\mathbf{S} = \mathbf{T}\mathbf{F}^{T}$, the kinematic equation (1), the divergence theorem, the constitutive relation and the equilibrium equation. This leads to

$$\int_{\mathcal{S}(t)} \mathbf{T}\mathbf{n}\cdot\mathbf{V}\,dA = \int_{\mathcal{R}_{\mathrm{R}}(t)} \frac{\partial}{\partial t}W(\mathbf{F})\,d\mathcal{V}_{\mathrm{R}} + \int_{\mathcal{S}_{\mathrm{R}}(t)} \mathbf{S}\mathbf{n}_{\mathrm{R}}\cdot\mathbf{F}\mathbf{n}_{\mathrm{R}}\,V_{\mathrm{R}}\,dA_{\mathrm{R}}. \tag{B.3}$$

The term representing the rate of change of the stored elastic energy in (B.1) can be written as

$$\frac{d}{dt}\int_{\mathcal{R}_{\mathrm{R}}(t)} W(\mathbf{F})\,d\mathcal{V}_{\mathrm{R}} = \int_{\mathcal{R}_{\mathrm{R}}(t)} \frac{\partial}{\partial t}W(\mathbf{F})\,d\mathcal{V}_{\mathrm{R}} + \int_{\mathcal{S}_{\mathrm{R}}(t)} W(\mathbf{F})\,V_{\mathrm{R}}\,dA_{\mathrm{R}}. \tag{B.4}$$

[7] In order to distinguish the symbol V_{R} used for the speed from that used for a referential volume element, we have used the symbol $d\mathcal{V}_{\mathrm{R}}$ for the latter.

Finally, from (A.15), the rate of increase of the surface energy can be written as

$$\frac{d}{dt}\int_{\mathcal{S}(t)} w(\lambda)\, dA = -\int_{\mathcal{S}(t)} (w+\lambda w')\left(\varkappa V - \frac{\partial U}{\partial s}\right) dA, \tag{B.5}$$

where the prime (in Appendix B) denotes differentiation with respect to λ. On substituting (B.2)-(B.5) into (B.1) we are led to

$$\mathbb{D} = \int_{\mathcal{S}_{\rm R}} \Big[\Delta\mu + \mathbf{S}\mathbf{n}_{\rm R}\cdot\mathbf{F}\mathbf{n}_{\rm R} - W(\mathbf{F})\Big] V_R dA + \int_{\mathcal{S}(t)} (w+\lambda w'-\sigma)\left(\varkappa V - \frac{\partial U}{\partial s}\right) dA. \tag{B.6}$$

In our two-dimensional setting, the surface energy *per unit reference area*, $\mathcal{W}(\lambda)$, is related to the surface energy per unit current area, $w(\lambda)$, by $\mathcal{W} = \lambda w$. Therefore the term between the first pair of parentheses in the second integral can be written as $\mathcal{W}'(\lambda) - \sigma$. In view of the constitutive equation $\sigma = \mathcal{W}'(\lambda)$ for the surface tension, see (8), the second integral in (B.6) drops out and we can write the dissipation rate as

$$\mathbb{D} = \int_{\mathcal{S}_{\rm R}} \Big[\Delta\mu + \mathbf{S}\mathbf{n}_{\rm R}\cdot\mathbf{F}\mathbf{n}_{\rm R} - W(\mathbf{F})\Big] V_R\, dA. \tag{B.7}$$

The speed $V_{\rm R}$ with which the referential boundary propagates is the volumetric flux of new material being added to the body. The factor multiplying it, i.e.,

$$f := \Delta\mu + \mathbf{S}\mathbf{n}_{\rm R}\cdot\mathbf{F}\mathbf{n}_{\rm R} - W(\mathbf{F}), \tag{B.8}$$

is therefore the conjugate driving force. Observe that the explicit effect of the surface tension has dropped out, but it still does affect the driving force implicitly through the stress, see (40) and (46).

Appendix C: Generalization to the Case Where the Stretch λ_1 is Permitted to be Extensional

The analysis in this paper can be readily extended to include stretches that are extensional. In this case the growth exponent ν is again given by (68). The curve of interest on the λ_1, K-plane on which $\nu = 0$ is now given by[8]

$$K = \mathcal{K}(\lambda_1), \quad 0 < \lambda_1 < 1/\lambda_{\rm Biot}, \tag{C.1}$$

where

$$\mathcal{K}(\lambda) := \frac{(\lambda^2+1)(1-\lambda^4)^2}{\lambda^2(1+\lambda^2+3\lambda^4-\lambda^6)}, \quad 0 < \lambda < 1/\lambda_{\rm Biot}. \tag{C.2}$$

This curve corresponds to the thick solid curve in Fig. 7. It declines monotonically on (0, 1), rises monotonically on $(1, 1/\lambda_{\rm Biot})$ and $\mathcal{K}(\lambda) \to \infty$ for both $\lambda \to 0^+$ and $\lambda \to 1/\lambda_{\rm Biot}$. Moreover, one finds that $\nu < 0$ on the shaded region above this curve which is therefore the region of stability of interest. Again, there is another region of this plane on which $\nu < 0$. This involves stretches that are more severe than those in the shaded region, and moreover is

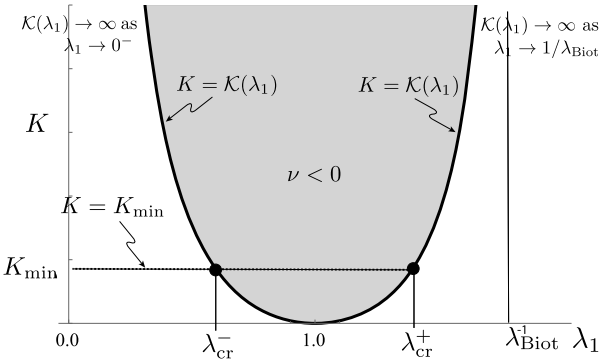

Fig. 7 The homogeneous solution corresponding to a value of $\lambda_1 \in (\lambda_{\rm cr}^-, \lambda_{\rm cr}^+)$ is stable for *all* wave numbers k. The critical values of the stretch $\lambda_{\rm cr}^{\pm}$ at instability are given by (C.3) where $\overline{\ell} = \sigma\kappa/G^2$

separated from the shaded region by a region of instability; see the corresponding discussion pertaining to Fig. 5.

The minimum value of K is again given by (73) and the horizontal straight line $K = K_{\rm min}$ on the λ_1, K-plane intersects the bold curve at two points as shown in Fig. 7. The corresponding values of stretch $\lambda_{\rm cr}^{\pm}$ are given by

$$K_{\rm min} = 2\big(\overline{\ell}\,\big)^{1/2} = \mathcal{K}(\lambda_{\rm cr}^{\pm}), \quad 0 < \lambda_{\rm cr}^- < 1 < \lambda_{\rm cr}^+ < 1/\lambda_{\rm Biot}, \tag{C.3}$$

where $\overline{\ell}$ was defined in (74). The discussion below (75) goes through again and we conclude that the homogeneous solution is stable against perturbations of all wave lengths provided $\lambda_{\rm cr}^- < \lambda_1 < \lambda_{\rm cr}^+$. The critical wave number, $k_{\rm cr} = \sqrt{\kappa/\sigma}$, is the same for both stretches $\lambda_{\rm cr}^-$ and $\lambda_{\rm cr}^+$.

Observe that when the stiffness $\kappa \to 0$ we have $\overline{\ell} \to 0$ and so $K_{\rm min} \to 0$ whence $\lambda_{\rm cr}^- \to 1$ and $\lambda_{\rm cr}^+ \to 1$; see Fig. 7. This agrees with the result in [4] concerning the case of a traction-free boundary. At the other extreme when $\kappa \to \infty$ one has $\overline{\ell} \to \infty$ and thus $K_{\rm min} \to \infty$ and therefore $\lambda_{\rm cr}^- \to 0^-$ and $\lambda_{\rm cr}^+ \to 1/\lambda_{\rm Biot}$. This agrees with the result in [4] pertaining to the case of growth on a smooth rigid surface.

Acknowledgements R.A. and E.P. gratefully acknowledge the support of the MIT-FVG Seed Fund. The work of G.T. and E.P. was supported by the Italian PRIN 2017 project "Mathematics of active materials: From mechanobiology to smart devices". G.T. and E.P. thankfully acknowledge the support of the Italian National Group of Mathematical Physics (GNFM-INdAM). G.T. acknowledges the Grant of Excellence Departments, MIUR, Italian Ministry of University and Research (Art.1, commi 314-337, Legge 232/2016).

Author contributions All authors contributed equally.

Funding Note Open Access funding provided by the MIT Libraries.

Declarations

Competing interests The authors declare no competing interests.

[8] Note that the denominator of $\mathcal{K}(\lambda)$ vanishes at $\lambda = 1/\lambda_{\rm Biot} \approx 1.84$.

References

1. Abeyaratne, R., Knowles, J.: On the driving traction acting on a surface of strain discontinuity in a continuum. J. Mech. Phys. Solids **38**(3), 345–360 (1990). https://doi.org/10.1016/0022-5096(90)90003-M
2. Abeyaratne, R., Knowles, J.K.: A note on the driving traction acting on a propagating interface: adiabatic and non-adiabatic processes of a continuum. J. Appl. Mech. **67**(4), 829–830 (1997). https://doi.org/10.1115/1.1308577
3. Abeyaratne, R., Knowles, J.K.: Evolution of Phase Transitions: A Continuum Theory. Cambridge University Press, Cambridge (2006)
4. Abeyaratne, R., Puntel, E., Tomassetti, G., Recrosi, F.: Surface accretion of pre-stretched half-space: Biot's problem revisited. J. Mech. Phys. Solids **167**, 104958 (2022). https://doi.org/10.1016/j.jmps.2022.104958
5. Ananthakrishnan, R., Ehrlicher, A.: The forces behind cell movement. Int. J. Biol. Sci. **3**(5), 303–317 (2007)
6. Asaro, R.J., Tiller, W.A.: Interface morphology development during stress corrosion cracking: Part I. Via surface diffusion. Metall. Mater. Trans. B **3**(7), 1789–1796 (1972). https://doi.org/10.1007/BF02642562. http://link.springer.com/10.1007/BF02642562
7. Bieling, P., Li, T., Weichsel, J., McGorty, R., Jreij, P., Huang, B., Fletcher, D., Mullins, R.: Force feedback controls motor activity and mechanical properties of self-assembling branched actin networks. Cell **164**(1), 115–127 (2016). https://doi.org/10.1016/j.cell.2015.11.057
8. Biot, M.A.: Surface instability of rubber in compression. Appl. Sci. Res., Sect. A **12**(2), 168–182 (1963). https://doi.org/10.1007/BF03184638
9. Bush, J.W.M.: 18.357: Interfacial phenomena, lecture 5, MIT Open Courseware (2010). https://ocw.mit.edu/courses/18-357-interfacial-phenomena-fall-2010/resources/mit18_357f10_lecture5/
10. Callen, H.: Thermodynamics and an Introduction to Thermostatistics, 2nd edn. Wiley, New York (1985)
11. Cameron, L.A., Footer, M.J., van Oudenaarden, A., Theriot, J.A.: Motility of acta protein-coated microspheres driven by actin polymerization. Proc. Natl. Acad. Sci. USA **96**(9), 4908–4913 (1999). https://doi.org/10.1073/pnas.96.9.4908
12. Chaudhuri, O., Parekh, S.H., Fletcher, D.A.: Reversible stress softening of actin networks. Nature **445**, 295–298 (2007). https://doi.org/10.1038/nature05459
13. Chen, Y., Yang, S., Wheeler, L.: Surface instability of elastic half-spaces by using the energy method. Proc. R. Soc. Lond. Ser. A **474** (2018). https://doi.org/10.1098/rspa.2017.0854
14. Dafalias, Y.F., Panayotounakos, D.E., Pitouras, Z.: Stress field due to elastic mass growth on spherical and cylindrical substrates. Int. J. Solids Struct. **45**(17), 4629–4647 (2008). https://doi.org/10.1016/j.ijsolstr.2008.03.029
15. Dafalias, Y.F., Pitouras, Z.: Stress field in actin gel growing on spherical substrate. Biomech. Model. Mechan. **8**(1), 9–24 (2009)
16. Dowaikh, M., Ogden, R.: On surface waves and deformations in a pre-stressed incompressible elastic solid. IMA J. Appl. Math. **44**, 261–284 (1990)
17. Freund, L.B.: A surface chemical potential for elastic solids. J. Mech. Phys. Solids **46**(10), 1835–1844 (1998). https://doi.org/10.1016/S0022-5096(98)00019-2
18. Fried, E., Gurtin, M.E.: The role of the configurational force balance in the nonequilibrium epitaxy of films. J. Mech. Phys. Solids **51**(3), 487–517 (2003). https://doi.org/10.1016/S0022-5096(02)00077-7
19. Grinfeld, M.A.: The stress driven instability in elastic crystals: mathematical models and physical manifestations. J. Nonlinear Sci. **3**(1), 35–83 (1993). https://doi.org/10.1007/BF02429859. http://link.springer.com/10.1007/BF02429859
20. van der Gucht, J., Paluch, E., Plastino, J., Sykes, C.: Stress release drives symmetry breaking for actin-based movement. Proc. Natl. Acad. Sci. USA **102**(22), 7847 (2005). https://doi.org/10.1073/pnas.0502121102
21. Gurtin, M.E.: Thermomechanics of Evolving Phase Boundaries in the Plane. Oxford University Press, London (1993)
22. Hutchinson, J.W.: Surface instabilities of constrained elastomeric layers subject to electro-static stressing. J. Mech. Phys. Solids **153**, 104462 (2021). https://doi.org/10.1016/j.jmps.2021.104462

23. John, K., Peyla, P., Kassner, K., Prost, J., Misbah, C.: Nonlinear study of symmetry breaking in actin gels: implications for cellular motility. Phys. Rev. Lett. **100**(6), 068101 (2008). https://doi.org/10.1103/PhysRevLett.100.068101
24. Kang, M., Huang, R.: Effect of surface tension on swell-induced surface instability of substrate-confined hydrogel layers. Soft Matter **22**, 5736–5742 (2010). https://doi.org/10.1039/c0sm00335b
25. Kestin, J.: A Course in Thermodynamics, Vol. II. McGraw Hill, New York (1979)
26. Mogilner, A., Keren, K.: The shape of motile cells. Curr. Biol. **19**(17), R762–R771 (2009). https://doi.org/10.1016/j.cub.2009.06.053
27. Mullins, W., Sekerka, R.: Stability of a planar interface during solidification of a dilute binary alloy. J. Appl. Phys. **35**(2), 444–451 (1964). https://doi.org/10.1063/1.1713333
28. Naghibzadeh, K., Walkington, N., Dayal, K.: Surface growth in deformable solids using an eulerian formulation. J. Mech. Phys. Solids **154**, 104499 (2021). https://doi.org/10.1016/j.jmps.2021.104499
29. Noireaux, V., Golsteyn, R.M., Friederich, E., Prost, J., Antony, C., Louvard, D., Sykes, C.: Growing an actin gel on spherical surfaces. Biophys. J. **78**(3), 1643–1654 (2000). https://doi.org/10.1016/S0006-3495(00)76716-6
30. Parekh, S.H., Chaudhuri, O., Theriot, J.A., Fletcher, D.A.: Loading history determines the velocity of actin-network growth. Nat. Cell Biol. **7**, 1219–1223 (2005). https://doi.org/10.1038/ncb1336
31. Prost, J., Joanny, J.F., Lenz, P., Sykes, C.: The physics of listeria propulsion. In: Lenz, P. (ed.) Cell Motility, Biological and Medical Physics, Biomedical Engineering, Chap. 1, pp. 1–30. Springer New York, New York, NY (2008). https://doi.org/10.1007/978-0-387-73050-9_1
32. Rafelski, S., Theriot, J.: Crawling toward a unified model of cell motility: spatial and temporal regulation of actin dynamics. Annu. Rev. Biochem. **73**, 209–239 (2004)
33. Skalak, R., Dasgupta, G., Moss, M., Otten, E., Dullemeijer, P., Vilmann, H.: Analytical description of growth. J. Theor. Biol. **94**(3), 555–577 (1982). https://doi.org/10.1016/0022-5193(82)90301-0
34. Tallinen, T., Biggins, J.S., Mahadevan, L.: Surface sulci in squeezed soft solids. Phys. Rev. Lett. **110**(2), 024302 (2013). https://doi.org/10.1103/PhysRevLett.110.024302. https://link.aps.org/doi/10.1103/PhysRevLett.110.024302
35. Tomassetti, G., Cohen, T., Abeyaratne, R.: Steady accretion of an elastic body on a hard spherical surface and the notion of a four-dimensional reference space. J. Mech. Phys. Solids **96**, 333–352 (2016). https://doi.org/10.1016/j.jmps.2016.05.015
36. Wu, C.H.: The chemical potential for stress-driven surface diffusion. J. Mech. Phys. Solids **44**(12), 2059–2077 (1996). https://doi.org/10.1016/S0022-5096(96)00059-2

Authors and Affiliations

Rohan Abeyaratne[1] · Eric Puntel[2] · Giuseppe Tomassetti[3]

✉ R. Abeyaratne
rohan@mit.edu

E. Puntel
eric.puntel@uniud.it

G. Tomassetti
giuseppe.tomassetti@uniroma3.it

1 Massachusetts Institute of Technology, Cambridge, MA, USA

2 Università di Udine, Udine, Italy

3 Università degli Studi Roma Tre, Roma, Italy